HOKKAIDO UNIVERSITY

Title	Structure Frustration Enables Thermal History-Dependent Responsive Behavior in Self-Healing Hydrogels
Author(s)	Yu, Chengtao; Cui, Kunpeng; Guo, Honglei; Ye, Ya Nan; Li, Xueyu; Gong, Jian Ping
Citation	Macromolecules, 54(21), 9927-9936 https://doi.org/10.1021/acs.macromol.1c01461
Issue Date	2021-11-09
Doc URL	http://hdl.handle.net/2115/87107
Rights	This document is the Accepted Manuscript version of a Published Work that appeared in final form in Macromolecules, copyright © American Chemical Society after peer review and technical editing by the publisher. To access the final edited and published work see https://pubs.acs.org/articlesonrequest/AOR-3F3VNBGEEDYUHSWCUNPN, see http://pubs.acs.org/page/policy/articlesonrequest/index.html.
Type	article (author version)
Additional Information	There are other files related to this item in HUSCAP. Check the above URL.
File Information	Macromolecules 54-21_9927-9936.pdf

Instructions for use

Structure Frustration Enables Thermal History-Dependent Responsive Behavior in Self-Healing Hydrogels

Journal:	*Macromolecules*
Manuscript ID	ma-2021-01461n.R2
Manuscript Type:	Article
Date Submitted by the Author:	n/a
Complete List of Authors:	Yu, Chengtao; Zhejiang University, CUI, KUNPENG; Hokkaido University , Faculty of Advanced Life Science GUO, HONGLEI; Hokkaido University , Faculty of Advanced Life Science Ye, Yanan; Hokkaido University, Faculty of Advanced Life Science LI, XUEYU; Hokkaido University , Faculty of Advanced Life Science Gong, Jian Ping; Hokkaido University , Faculty of Advanced Life Science

SCHOLARONE™
Manuscripts

1
2
3
4
5
6
7
8
9
10
11
12
13
14
15
16
17
18
19
20
21
22
23
24
25
26
27
28
29
30
31
32
33
34
35
36
37
38
39
40
41
42
43
44
45
46
47
48
49
50
51
52
53
54
55
56
57
58
59
60

Structure Frustration Enables Thermal History-Dependent Responsive Behavior in Self-Healing Hydrogels

Chengtao Yu[a,b], Kunpeng Cui[c]*, Honglei Guo[d], Ya Nan Ye[e], Xueyu Li[e], and Jian Ping Gong[c,d,e]*

[a]Graduate School of Life Science, Hokkaido University, Sapporo 001-0021, Japan; [b]Institute of Zhejiang University-Quzhou, 78 Jiuhua Boulevard North, Quzhou 324000, China; [c]Institute for Chemical Reaction Design and Discovery (ICReDD), Hokkaido University, Sapporo 001-0021, Japan; [d]Faculty of Advanced Life Science, Hokkaido University, Sapporo 001-0021, Japan; [e]Global Institution for Collaborative Research and Education (GI-CoRE), Hokkaido University, Sapporo 001-0021, Japan.

*Corresponding authors:
Kunpeng Cui, E-mail: kpcui@sci.hokudai.ac.jp
Jian Ping Gong, E-mail: gong@sci.hokudai.ac.jp

Abstract: Biological soft tissues usually execute their functions via nonequilibrium and dynamic structural transformations. By contrast, functional hydrogels are mainly constructed by implementing static and equilibrium structures in the polymer network. Herein, using polyampholyte hydrogel as a model system, we demonstrated that the nonequilibrium structure transformation in self-healing hydrogels enables the gels many new features, including thermal history dependence, quick and asymmetric

1

thermal response (instant transparent-to-turbid transition but slow turbid-to-transparent transition), tunable cloud point, tunable recovery time, tiny changes in sample size and mechanical performance. These features make them distinct to conventional thermoresponsive hydrogels based on thermodynamic equilibrium and endow them a new type of promising thermoresponsive materials. We revealed the structure change and studied the role of the thermal protocol on this thermoresponsive behavior by combining ultraviolet spectrum, small-angle X-ray scattering, rheology, and mechanical measurements. We also presented two conceptual applications of this thermoresponsive hydrogel in thermal imaging and security paper. We believe that this work will inspire future research on creating functional hydrogels via nonequilibrium structure transformations.

Introduction

Biological soft tissues and hydrogels have similar soft and wet nature.[1] Biological soft tissues possess complex but elegant structures and excellent functionalities.[2,3] The functions of biological tissues are usually executed via nonequilibrium structure transformations. For example, the brain acquires information by forming cellular memory traces and increases the synaptic size of engram cells, and these changes become the part of neural code for memory.[4,5] The information recorded and stored in the brain spontaneously forgets over time, and this occurs simultaneously with the erosion in cellular memory trace and the decrease in synaptic size. By contrast, hydrogels are usually amorphous and have poor functionalities.[6,7] Efforts have been made toward fabricating hydrogels with functionalities by implementing ordered structures into hydrogel networks, which endow the gels with robust functionalities, such as structural color,[8–10] stimuli-responsive behavior,[11–13] and mechanical strength.[14–16] However, the ordered structures in hydrogels are usually in equilibrium or quasi-equilibrium states, distinctly different from the nonequilibrium and dynamic structures in biological tissues. Introducing nonequilibrium structure into hydrogels to realize unique functionalities is seldom realized.

Recently, we reported that tough and self-healing hydrogels possess a dynamic memorizing-forgetting function via a nonequilibrium structure transformation, in analogy to human brain.[17] The hydrogels containing abundant dynamic bonds can memorize two-dimensional (2D) information via thermal learning, and the memorized information spontaneously forgets with time. The forgetting time is proportional to

3

the learning time or learning strength. This dynamic memorizing-forgetting behavior of hydrogels is realized by the asymmetric swelling/shrinking kinetics, as well as the transparency change of the gel caused by structure frustration upon cooling. Such dynamic memorizing-forgetting behavior is observed in many self-healing hydrogels containing physical bonds, for example, polyampholyte (PA) hydrogels with different chemical compositions and hydrogen-bonding hydrogels, independent of gel chemistry.[17]

The thermoresponsive behavior of hydrogels containing abundance of physical bonds enabled by nonequilibrium structure transformation is distinctly different from that of traditional thermoresponsive hydrogels, although traditional thermoresponsive hydrogels also show strong asymmetric swelling/shrinking kinetics and transparent/turbid transition.[18–22] The first difference is that the transparent/turbid transition occurs only at a characteristic temperature specific to the materials for traditional thermoresponsive hydrogels, however, it occurs at any temperature for hydrogels containing many physical bonds provided the temperature difference is sufficient upon cooling. The second difference is that the volume change in conventional thermoresponsive hydrogels is ten or hundred folds at the characteristic temperature, while it is only in the percentage scale in gels containing abundance of physical bonds.

Herein, we attempted to understand, in-depth, this unusual thermoresponsive behavior and focused on the following questions: (1) what is the structure change behind the thermoresponsive behavior? (2) why is the size change of the gel minimal?

4

(3) how do the cooling degree and cooling rate influence the transparent/turbid transition? (4) what is the difference in mechanical performance between transparent and turbid gels? Finally, we conceptually demonstrate the applications of this unusual thermoresponsive behavior in thermal imaging and security paper.

Results and discussion

Thermal history-dependent responsive behavior. Conventional thermoresponsive hydrogels are usually characterized by a sharp phase transition at a temperature defined as the lower critical solution temperature (LCST)[23–25] or upper critical solution temperature (UCST)[26–29]. In case of LCST-type gels, the polymers below the LCST are water-soluble and in swollen state. However, those polymers，above the LCST, are less or not water-soluble and in a collapsed form[30]. Such a change in the solubility of the polymer is usually featured by a transparent/turbid transition in optical appearance and dramatic changes in the size and mechanical performance of the gel [31–33]. These changes require a relatively long time, which increases with the gel size, and are governed by a water-diffusion controlled process. The UCST-type gels exhibit a similar thermoresponsive behavior but with opposite temperature dependence[34,35]. The phase transition temperature of either LCST or UCST type gels, governed by thermodynamics, is uniquely determined by the chemical structure of the polymer comprising the gels. Here, we adopted a polyampholyte hydrogel (PA gel)[36] as a model system, to illustrate that the thermoresponsive behavior of self-healing hydrogels enabled by structure frustration is markedly different from the thermoresponsive behavior of traditional hydrogels.

5

The PA gels were prepared by radical copolymerization of anionic monomers, sodium *p*-styrenesulfonate (NaSS), and cationic monomers, methyl chloride quarternized *N,N*-dimethylamino ethylacrylate (DMAEA-Q), in a concentrated aqueous solution with a total monomer concentration of 2.5 M at the charge balanced point. According to a recent work[37], the obtained polymer chains have NaSS rich sequences and DMAEA-Q rich sequences (Fig. S1), due to the difference in the reactivity ratios of these two monomers during copolymerization (for details see SI). The P(NaSS-co-DMAEA-Q) hydrogel is amorphous, as confirmed by the differential scanning calorimetry result (Fig. S2). The gel equilibrated in pure water has a water content of 46 wt%, and it is tough and self-healable because of the reversible nature of the dynamic ionic bonds. Sheet-shaped gels with a thickness approximately 1.2 mm were used in the following experiments without special mention.

Fig. 1a presents an example of the transparency change in a PA gel having the following thermal history. The gel was initially equilibrated in a cold-water bath with a temperature T_F = 25 °C (original gel); then, the gel was transferred to a hot-water bath with a temperature T_L = 80 °C and maintained at this temperature for t_L = 2 h (heated gel); thereafter, the gel is returned to the cold bath with T_F = 25 °C. Here, the subscripts L and F stand for learning and forgetting, respectively, following the notations adopted in our previous work, in which we mimicked the learning and forgetting process of the human brain using such a non-equilibrium thermal process.[17]
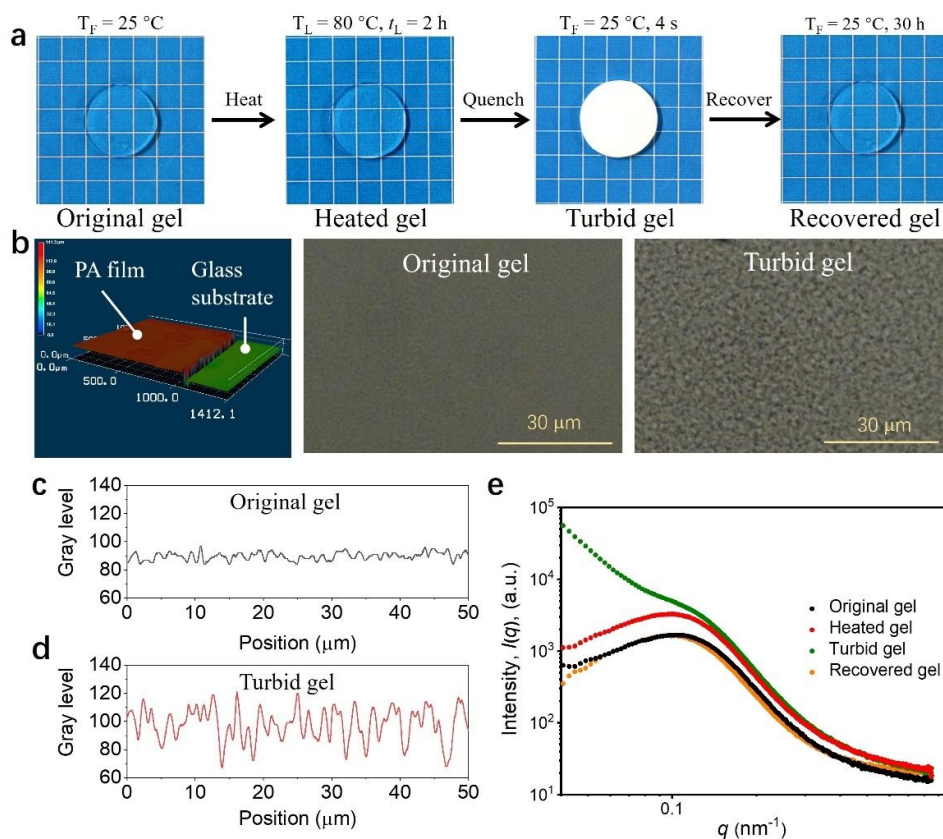
Fig. 1. Transient thermal history-dependent response of polyampholyte hydrogel (PA gel) containing abundant ionic bonds. The gel is initially transparent at a low temperature T_F (original gel), and the transparency keeps when heating to a high temperature T_L for a time t_L (heated gel). Upon being cooled suddenly to the low temperature T_F, the gel first becomes turbid very quickly (turbid gel); then gradually turns to transparent over a long time (recovered gel). (a) Optical image of original, heated, turbid, and recovered gel with a thermal history of $T_F = 25\ °C$, $T_L = 80\ °C$ and $t_L = 2$ h. Background lattices: 5 mm. The thickness of the gel is about 1.2 mm. (b) 3D laser microscope image of the thin original PA film, and microscope images of the original gel and turbid gel. The gel thickness is about 50 μm. The gel has a thermal history of $T_F = 25\ °C$, $T_L = 60\ °C$ and $t_L = 1$ min. (c, d) 8-bit grayscale (GS) of the microscopy images as a function of position of the (c) original and (d) turbid gels, where GS = 0 means "black" and GS = 255 means "white". (e) Small-angle X-ray scattering profiles to show the internal structure change of the gel during the thermal response process. The gel has a thermal history of $T_F = 25\ °C$, $T_L = 80\ °C$, and $t_L = 2$ h.

The original gel at 25 °C water bath was transparent, and it maintains the transparency during heating at 80 °C (Figs. 1a and S3). When the gel was cooled to 25 °C, it turned to turbid instantly (turbid gel). The turbid gel spontaneously

recovered to transparent (recovered gel) over a considerable period (30 h, Figs. 1a and

S4). The transparency change of the PA gel was caused by sudden cooling, and it

recovered to transparent slowly, which is different from the LCST or UCST type gels

where the transparency only depends on temperature after reaching equilibrium,

independent of time.[27,30] This difference arises from the fact that, the transparency

change of PA gel at cooling is caused by frustrated structure formation[17], while the

transparency change in the conventional thermoresponsive gel is caused by the

hydrophobicity/hydrophilicity change in the polymer chains with temperature[27,30].

PA gels containing an abundance of ionic bonds have strong ionic interactions.

When the gel is heated from T_F to T_L, the gel swells slightly by absorbing water. By

cooling the gel suddenly from T_L to T_F, the temperature of the gel decreases quickly,

while the excess amount of absorbed water cannot be expelled out of the gel instantly.

Therefore, the water molecules are locally trapped between the aggregated polymers

to form a transient frustrated structure.[17] Two strongly asymmetric processes are

involved in this thermoresponsive behavior. The first is the large kinetic difference in

thermal diffusion and water diffusion upon cooling, exhibited as a 3-order difference

in their diffusion coefficients (Table 1)[17]. This large kinetic difference causes

structure frustration, which results in the second large kinetic difference between

swelling and shrinking. For example, the gel swelling at 80 °C has a diffusion

coefficient, D_{sw} of $\sim 10^{-10}$ m^2/s, while the gel shrinking at 25 °C has a diffusion

coefficient, D_{sh} of $\sim 10^{-12}$ m^2/s.[17]

8

Diffusion coefficient	Value (m^2/s)
D_{th}	~10^{-7}
D_{sw}	~10^{-10}
D_{sh}	~10^{-12}

Table 1. Thermal diffusion coefficient, D_{th} at 25 °C, swelling diffusion coefficient, D_{sw} at 80 °C, and shrinking diffusion coefficient, D_{sh} at 25 °C. These values were taken from the ref[17].

Structure change. To reveal the structure change behind this unusual thermoresponsive behavior, we performed microscopic observation of a PA gel film (50 μm thick) upon cooling (Fig. 1b). The original transparent gel exhibited a homogeneous appearance on the observation length scale. The gel was heated at 60 °C to reach equilibrium and then cooled to room temperature (25 °C). Upon sudden cooling to room temperature, microphase separation with a structural length of about 3 μm occurred (Figs. 1c and 1d), which explains the turbid appearance of the gel. The microphase separation structure gradually disappeared with time until the gel reached an equilibrium state at room temperature. The small-angle X-ray scattering (SAXS) results are consistent with the microscopy observations, which further support this mechanism (Fig. 1e). The SAXS profile of the original gel equilibrated at room temperature has a scattering peak at q around 0.1 nm^{-1}, resulting from the nanoscale phase-separated structure of PA gels, which is composed of a soft phase and a hard phase with a structure length of approximately 60 nm[38–42]. The scattering peak was maintained in the heated gel, but the peak position shifted slightly to a small

9

q, and the peak intensity increased compared with those of the original gel, due to the increased phase contrast and increased structure length caused by water absorption. During swelling, the soft phase absorbs more water than the hard phase, because of its lower stiffness relative to the hard phase, resulting in a larger phase contrast of the heated gel. Different from the original gel and heated gel, the turbid gel obtained by sudden cooling exhibited a sharp increase in scattering intensity in the small *q* region, suggesting the formation of large-scale structure, consistent with microscopic observation of the appearance of microphase separation. The SAXS profile of the gel recovered from turbid to transparent is almost the same as the original gel, suggesting that not only the transparency but also the nano-scale internal structure recovered to the initial state. As revealed in our previous study[17], the contents of bound water in the original and turbid gels are almost the same, while the content of free water increased in the turbid gel, suggesting that the microphase separation was caused by the local aggregation of free water. These water aggregates are energetically unfavorable and gradually diffuse out of the gel, resulting in the spontaneous recovery of both structure and appearance.

Small size change. The size change of the PA gel during thermal response is exceedingly small. The size of the gel after heating at $T_L = 80$ °C for $t_L = 2$ h was just 1.08 times that of the gel equilibrated at 25 °C; for $T_L = 40$ °C, it decreases to 1.02 (Figs. 2 and S5). The small size change of the PA gel during thermal response is in stark contrast to that of the conventional LCST or UCST type gels, where the volume changes dramatically, up to ten or hundred of times.[23–25,34,35] For comparison, we also

studied the size change of a non-thermoresponsive polyacrylamide (PAAm) hydrogel. The equilibrated size of this gel after heating at T_L = 80 °C was just 1.003 times that equilibrated at 25 °C, that is, it was of the same order as the size change due to the thermal expansion of water.[43]

Before discussing the swelling behavior of PA gels, we discuss the effect of temperature on the swelling behavior of the thermoresponsive and non-thermoresponsive hydrogels. The swelling equilibrium of a hydrogel without charges is a balance of two contributions: $\Delta F_{mix} = k_B T \frac{V}{v_{site}}(1-\phi)[\ln(1-\phi) + \chi\phi]$ from the mixing of the polymer and solvent to promote the swelling of the gel, and $\Delta F_{ela} = \frac{3k_B T}{2} \frac{V\phi}{N_x v_{site}}(1-\phi)\left[\left(\frac{\phi_0}{\phi}\right)^{2/3} - 1 - \frac{1}{3}\ln\left(\frac{\phi_0}{\phi}\right)\right]$ from the elasticity of the gel network to suppress gel swelling.[44,45] Here, k_B is the Boltzmann's constant, T the absolute temperature, V the gel volume, v_{site} the lattice site volume, N_x the average number of monomers between crosslinks, ϕ the polymer volume fraction, ϕ_0 the polymer volume fraction at the prepared state, and χ is the polymer-solvent interaction parameter. For thermoresponsive hydrogels, χ changes significantly with temperature, leading to dramatic changes in ΔF_{mix} and thus in volume at a critical temperature. For the non-thermoresponsive hydrogels such as the PAAm gel, the temperature dependence of χ is very weak. Thus, both ΔF_{mix} and ΔF_{ela} are linearly related to temperature T. Consequently, changing the temperature has a negligible effect on the swelling equilibrium of the gel.
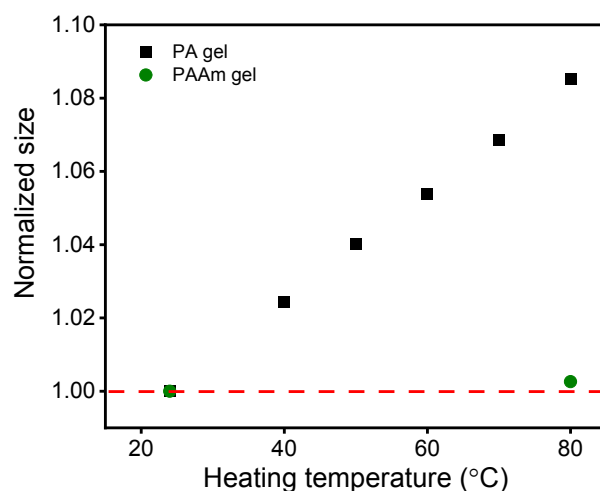
Fig. 2. Normalized size change of the PA gel and PAAm gel relative to the original (equilibrated at 25 °C) versus heating temperature. The gels were heated at different temperatures for t_H = 2 h to reach equilibrium.

For the swelling equilibrium of PA hydrogels, two additional contributions must be considered: ΔF_{trans} from the translational energy of small ions and $\Delta F_{Coulombic}$ from the Coulombic interaction of the charges.[45] The PA gel studied in this work has balanced charges in the polymer chains, thus, ΔF_{trans} is negligible. Therefore, ΔF_{mix} and ΔF_{ela} were balanced by $\Delta F_{Coulombic}$. Considering that there is no dramatic size change during the thermal response and the thermal response can occur at any temperature upon cooling, χ should be almost independent of temperature, T. In this case, ΔF_{mix} and ΔF_{ela} are both linearly related to temperature T. On the other hand, the Coulombic contribution, $\Delta F_{Coulombic}$, is inversely proportional to the dielectric constant, ε, of water. ε decreases with increasing temperature in a nonlinear way. Therefore, $\Delta F_{Coulombic}$ increases with temperature but not linearly. Since the temperature effect on ΔF_{mix} and ΔF_{ela} and the temperature effect on $\Delta F_{Coulombic}$ are not fully matched, the gel needs to reach a new swelling equilibrium when changing

12

temperature. Specifically, for a temperature change from 25 °C to 80 °C, the relative temperature change $\Delta T/T$ = (298K - 353K)/298K = -0.185 and dielectric constant change $\Delta\varepsilon/\varepsilon$ = ($\varepsilon_{25°C}$ - $\varepsilon_{80°C}$)/$\varepsilon_{25°C}$ = 0.22 are almost canceled using $\varepsilon_{25°C}$ = 78.3 and $\varepsilon_{80°C}$ = 61.0.[46] This explains the small volume change of the gel with temperature.

Effects of heating time, t_L, heating temperature, T_L, and cooling temperature T_F. The degree of turbidity of the PA gel immediately after cooling, as characterized by the transmittance, is determined by the thermal history. The appearance of the PA gels with different t_L ranging from 0 to 10 min, after jumping temperature from T_L = 60 °C to T_F = 25 °C for 1 min, is shown in Fig. 3a. The original gel (t_L = 0 min) is transparent; by increasing t_L to 1 and 3 min, the gels become semitransparent; Further increasing t_L, the gels turn to opaque. The transmittance of these gels decreased gradually with increasing t_L (Fig. 3b). Here, we should mention that the turbidity can only be tuned for the gel before reaching swelling equilibrium at T_L, and further increase of t_L after reaching swelling equilibrium has no effect on the turbidity change. This is because, before reaching swelling equilibrium, the water absorption increases with t_L, starting from the surface layer to the inner layer of the gel. Increasing t_L leads to a thicker opaque layer, and thus a higher degree of turbidity of the gel. The degree of turbidity of the PA gel, immediately after cooling, can also be tuned by tuning T_L or T_F. Increasing T_L or decreasing T_F has a similar effect as increasing t_L (Fig. S6).
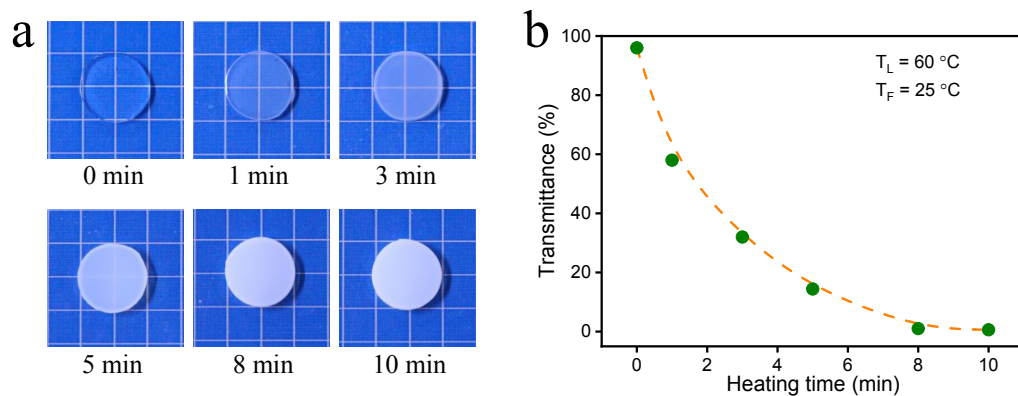
Fig. 3. Effect of heating time on the transmittance of PA gels. (a) Optical images and (b) transmittance of PA gels at cooling versus heating time t_L. The gels were heated at $T_L = 60$ °C for a certain time, t_L, and thereafter transferred to a cold bath with a T_F of 25 °C. t_L changed from 0 to 10 min. The transmittance was measured at 1 min after the samples were transferred to the cold bath. Background lattices in (a), 5 mm.

Effects of cooling degree and cooling rate. Since the turbidity change of the PA gel is a transient phenomenon due to the excess water content, the PA gel exhibits no characteristic temperature for the transparent/turbid transition, which is different from conventional thermoresponsive gels where the phase transition occurs at a temperature characteristic to the gels.[27,30,35] To study what cooling degree is needed for the transparent/turbid transition, PA gels were equilibrated at different temperatures ranging from 80 to 40 °C; then, they were cooled at a cooling rate of 1 °C/min to check the temperature where the transparent/turbid transition occurs.
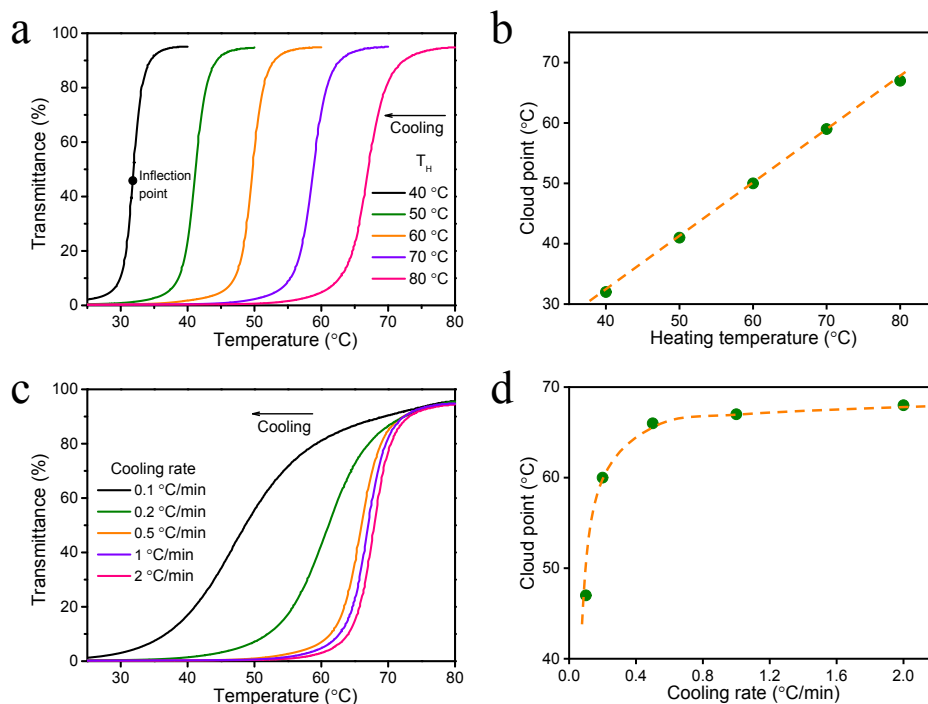
Fig. 4. Effect of the cooling degree and cooling rate on the cloud point. (a) Transmittance and (b) cloud point of PA gels during cooling at a cooling rate of 1 °C/min. The gels were initially equilibrated at T_F = 25 °C and then heated to different T_L for t_L = 2 h before measurement. The cloud point is defined by the inflection point of the transmittance curve. (c) Transmittance change and (d) cloud point of PA gels during cooling at different cooling rates. The equilibrated gels at T_F = 25 °C were heated to T_L = 80 °C for t_L = 2 h before measurement.

The gels heated at different temperatures were transparent, and their transmittances are similar (Fig. S7). During cooling, the gel initially heated at a higher T_L became turbid at a relatively higher temperature, and *vice versa* (Fig. 4a). To quantify this process, we used the temperature at the inflection point of the transmittance curve as the cloud point (Fig. 4a). For the gels that were initially heated at T_L = 80, 70, 60, 50, and 40 °C, their cloud points were 67, 59, 50, 41, and 32 °C, respectively, at a cooling rate of 1 °C/min. The cloud point almost linearly increases with the initial heating temperature T_L (Fig. 4b), suggesting that the transparent-to-turbid transition occurs at

15

a certain cooling degree for a constant cooling rate (for example, approximately 10 °C

at a cooling rate of 1 °C/min). This phenomenon is consistent with our analysis that

the driving force for swelling/deswelling upon changing the temperature depends on

the temperature difference rather than the absolute temperature.

As the turbidity change is a transient phenomenon, the cooling rate also influences

the cloud point. To study this effect, PA gels were initially heated at 80 °C and then

cooled at different rates (Fig. 4c). The cloud point first increased strongly with the

cooling rate and then remained constant (Fig. 4d). The transition point is around

0.5 °C/min. The turbidity change of the gel during cooling is a competition between

the formation of frustrated structure by local water aggregations and the suppression

of structure frustration by expelling the water out of the gel. As the driving force for

frustrated structure formation depends on the temperature difference, while the expel

of water depends on the diffusion time, thus a slower cooling rate leads to a lower

cloud point. Here we can surmise why the transition of the cloud point against the

cooling rate occurs at a cooling rate of 0.5 °C/min. The gel thickness, *d,* we used here

is ~1 mm, and the characteristic water diffusion time τ of this gel can be estimated

from the relation $\tau = \frac{d^2}{D_{sw}\pi^2}$. For a D_{sw} of 10^{-10} m²/s, τ is about 1000 s. As discussed

above, a 10 °C temperature difference is required for the transparent/turbid transition

under fast cooling. With a cooling rate of 0.5 °C/min, a 10 °C cooling needs 1200 s,

which is almost the same to the characteristic water diffusion time. Therefore, at a

cooling rate below 0.5 °C/min, water diffusion out of the gel starts to match the

temperature change, which gives a strong dependence of the cloud point on the

16

cooling rate.

Recovery process. The turbid gel after cooling is unstable and recovering to transparent automatically, which is also distinct to the conventional thermoresponsive gels in which the turbidity does not change once the temperature is constant. Fig. 5a illustrates the transparency change of a PA gel during the recovery process with different heating time t_L. T_L and T_F were maintained at 60 °C and 25 °C, respectively. The time for the turbid gel to revert to transparent, denoted as recovery time or forgetting time t_F, first increased with the heating time t_L and then remained constant around a heating time of 100 min (Fig. 5b). This indicates that after a heating time around 100 min, the gel reached swelling equilibrium. Further increasing the heating time had no influence on the recovery time. The recovery time t_F was significantly longer than the heating time. In the unsaturated heating time region, the ratio t_F/t_H is about 22, indicating a strong asymmetry between the swelling and deswelling kinetics.

The recovery time also depends on the heating temperature, T_L. For a heating time t_L of 2h and a cooling temperature T_F of 25 °C, the recovery time almost linearly increased with heating temperature T_L (Figs. 5c and 5d). The recovery process has been studied in our previous work[17], therefore, we do not discuss this aspect in detail herein.
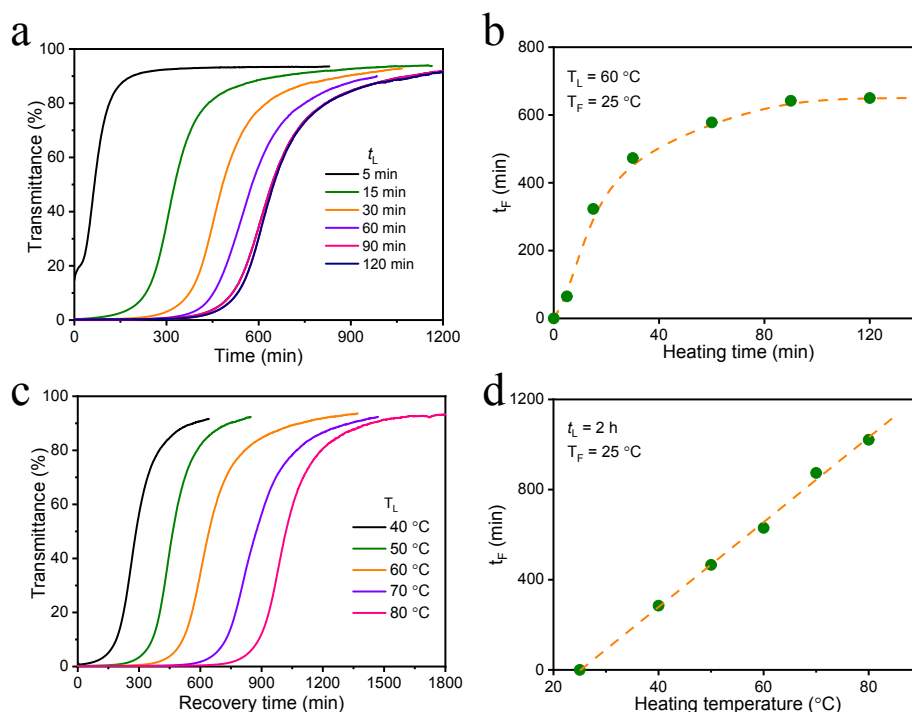
17

Fig. 5. Opaque/transparent transition of PA gels during recovery. (a) Transmittance change and (b) recovery time or forgetting time, t_F, in the recovery process of PA gels with different heating time or learning time t_L. T_L and T_F are 60 and 25 °C, respectively. The characteristic recovery time is defined by the inflection point of the transmittance curve. (c) Transmittance change and (d) characteristic recovery time in the recovery process of PA gels at different heating temperatures, T_L. t_L and T_F are 2 h and 25 °C, respectively.

Negligible change in mechanical performance. Although the structure and the transparency are distinctly different for the PA gels in equilibrium and nonequilibrium states, their mechanical performances are not clearly different. First, we compared their dynamic response in small strain range. Fig. 6a represents the frequency dependence of the storage modulus G' and loss modulus G'' from 0.1 to 100 Hz of the gel equilibrated at 25 °C (transparent gel) and the gel immediately after cooling to 25 °C after having been heated at 80 °C for 2 h (turbid gel). Although the PA gel recovers to transparent gradually during the measurement, the recovery time (30 h,

Fig. 1a) is much longer than the mechanical measurement time (several seconds or minutes). Thus, the structure change during the mechanical measurement is negligible. The transparent gel and turbid gel exhibit almost the same frequency dependence of G' and G'', suggesting that the two gels have almost the same small strain dynamic behavior.
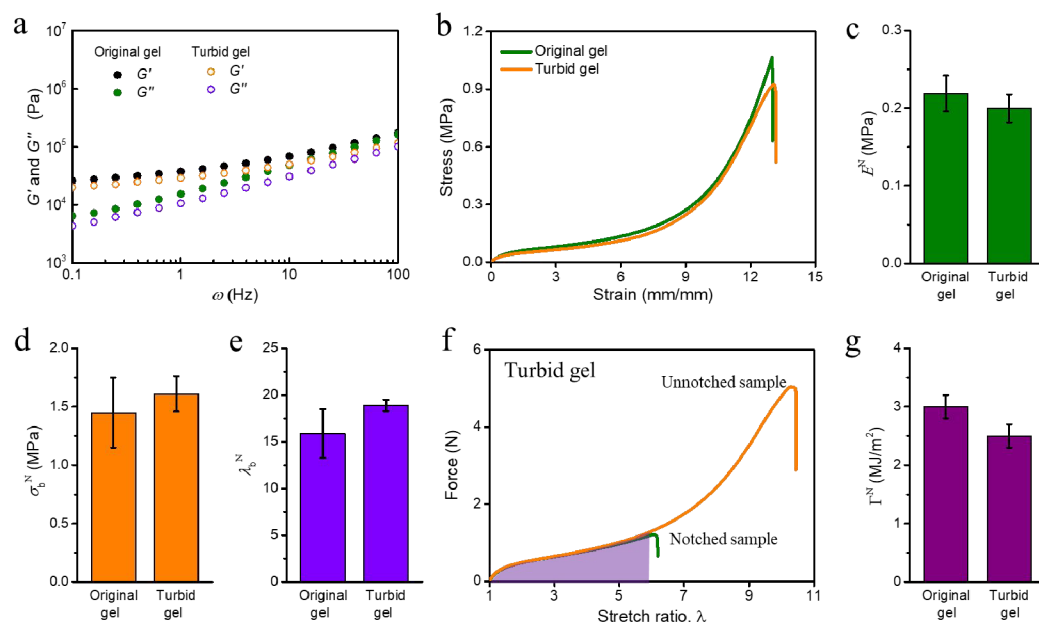

Fig. 6. Mechanical performances of the original and turbid gels. (a) Frequency dependence of the storage modulus G' and loss modulus G'' at 25 °C. (b-e) Uniaxial tensile test: (b) Nominal stress-strain curves, (c) Young's modulus E^N, (d) fracture stress σ_b^N, and (e) fracture stretch ratio λ_b^N after removing the polymer density effect caused by the size change of the gel. (f) Force-stretch ratio (λ) curves of notched and unnotched samples for the turbid gel. (g) Fracture energy Γ^N of the original gel and turbid gel after removing the polymer density effect caused by the size change of the gel. The gels were initially equilibrated at $T_F = 25$ °C and then heated to $T_L = 80$ °C for $t_L = 2$ h. The measurements were performed immediately after moving the gels back to the $T_F = 25$ °C water bath.

PA gels are viscoelastic, as demonstrated by their rheology behavior. We chose a specific rate to compare the large-strain uniaxial tensile behavior of the transparent gel and turbid gel. Fig. 6b exhibits the stress-strain curves of the original gel and the turbid gel with an initial strain rate of 0.14 s^{-1} at 25 °C. Figs. 6c-e exhibit the

19

calculated Young's modulus, E^N, fracture stress, $\sigma_b{}^N$, and fracture stretch ratio, $\lambda_b{}^N$,

after removing the polymer density effect caused by the small size change (for details

see SI, Figs. S8-10). Their E^N, as well as $\sigma_b{}^N$ and $\lambda_b{}^N$, have no obvious difference. We

further measured the fracture energy Γ, a parameter to characterize the toughness of

materials, of the transparent gel and turbid gel (Fig. 6f). Γ of the two gels after

polymer density correction (Γ^N) are also nearly the same (Fig. 6g). The negligible

change in the mechanical performance of the PA gel before and after the formation of

the nonequilibrium structure can be rationalized by the following reason. The

nonequilibrium structure is caused by the local aggregation of free water at μm scale

(Fig. 1b), while the skeleton bicoutinuous network structure of the gel at 60 nm scale

did not significantly change (Fig. 1e). Tough and soft hydrogels are usually

insensitive to flaws up to a length scale of millimeters and even centimeters.[47]

Therefore, the mechanical performance of the PA gel is insensitive to local water

aggregations in the μm range. We further confirmed this by introducing a flaw with a

diameter of 0.25 mm in the PA gels and demonstrated that this flaw indeed had a

negligible influence on the mechanical performance (Fig. S11).

Applications of the thermoresponsive behavior. As demonstrated above, the

thermoresponsive behavior of the PA gel arising from structure frustration has many

new features: thermal history dependence, quick and asymmetric thermal response

(instant transparent-to-turbid transition but slow turbid-to-transparent transition),

tunable cloud point, tunable recovery time, tiny changes in sample size, and

mechanical performance. These features distinguish them from conventional

thermoresponsive hydrogels and endow them with a new type of promising

thermoresponsive materials. Herein, we present two conceptual applications of this
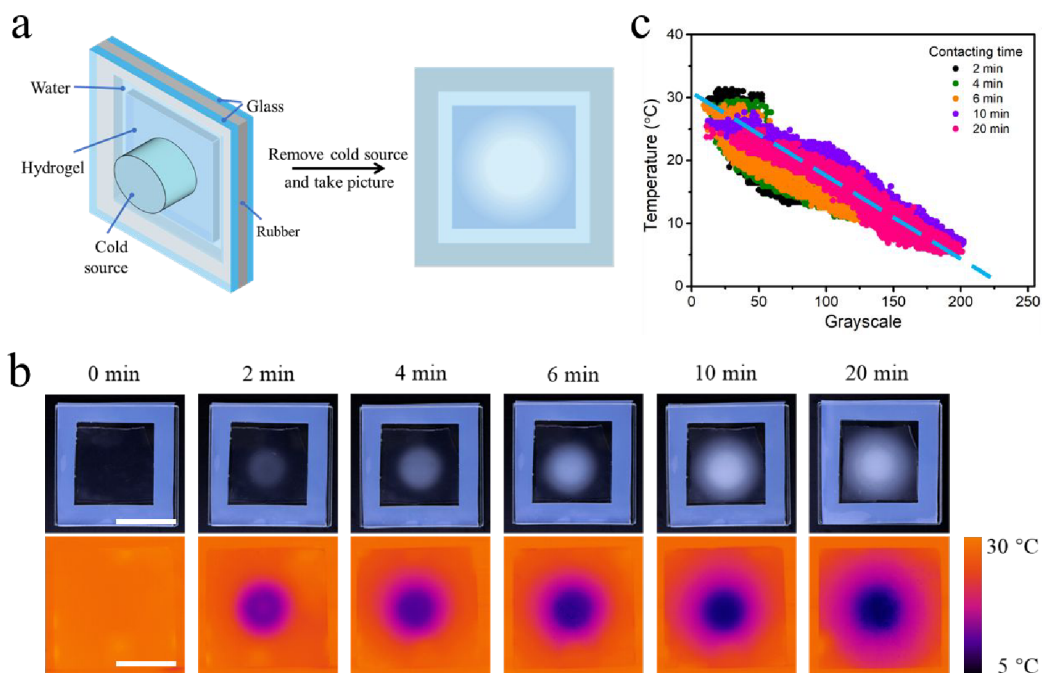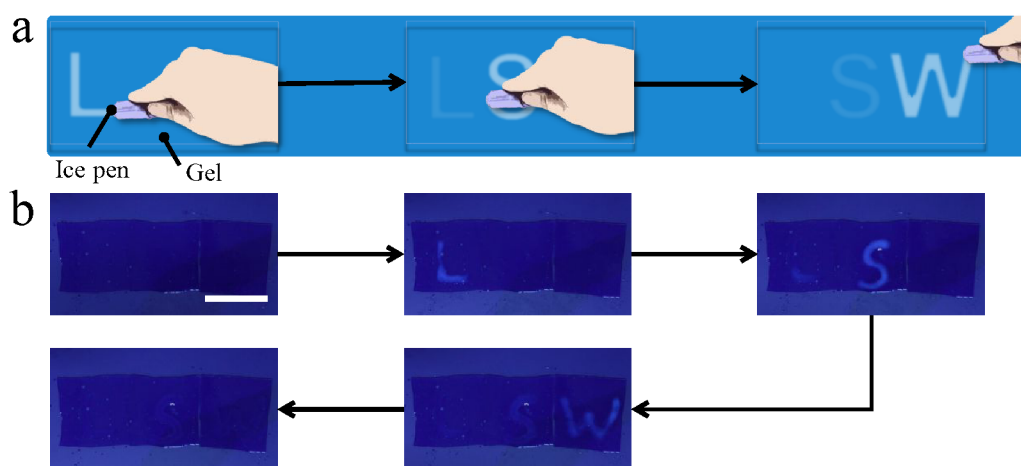
thermoresponsive behavior.

Fig. 7. Application of the thermoresponsive behavior of PA gel in 2D thermal imaging. (a) Scheme to show the experimental procedure: A PA gel with a thickness of 1.2 mm was sealed in a water chamber consisting of two transparent glasses separated by a rubber spacer; then, one surface of the sealed sample was attached to a cylindrical cold source (diameter of 35 mm) and a constant temperature of 5 °C; after contacting with a certain time, the cold source was removed, and the optical and infrared images were taken immediately. (b) Optical (upper) and infrared (lower) images of the sealed sample with different contacting time. The infrared images were taken by an infrared thermometer (Optris, Germany), and the working distance was approximately 25 cm. (c) Relationship between the turbidity and temperature of gels with different contacting time. The turbidity is represented by the 8-bit grayscale (GS) of the optical image, where GS = 0 means "black" and GS = 255 means "white". Scale bars: 5 cm.

One application of the gels is in 2D thermal imaging. As shown in Fig. 7a, a PA gel

was sealed in a water chamber comprising two glass sheets separated by a rubber

spacer. We putted a cylindrical cold source (diameter of 35 mm) with a constant

temperature of 5 °C on the center of the chamber to cool the gel. After a certain

contacting time, we removed the cold source and immediately captured the optical

and infrared images of the sealed sample. Fig. 7b shows the optical and infrared

images of the gels at different contacting time between the cold source and sealed gel,

respectively. The temperature decreases along the radial direction from the center of

the gel owing to heat transfer. This temperature gradient is well represented by the

turbidity change of the gels from the center to the edge. Quantitative analysis shows

that the temperature and the turbidity nearly have a linear relationship (Fig. 7c),

consistent with the results obtained in Fig. 4b. This result suggests that the PA gel has

potential in thermal imaging, where the transparency of images can be directly used to

reflect the temperature distribution.

Fig. 8. Application of the thermoresponsive behavior of PA gel as a security paper for temporarily recording of information. (a) Scheme to show the experimental procedure for recording information and the autonomic disappearance of information: An ice stick, serving as a pen, is used to write information on the surface of the PA gel. As the ice temperature (0 °C) is much lower than the gel temperature (around 25 °C) and the contacting time is short, the ice pen writing displays white characters, but the white characters quickly disappear. (b) An example to show the autonomic disappearance of the recorded information on the PA gel. A letter "L" is initially written on the surface of the gel; after 30 s, "S" is written, during which time and L gradually disappears; then, "W" is written after waiting for another 30 s, and S almost

disappears; finally, W also disappears, and the PA gel reverts to transparent as blank. Scale bars: 5 cm.

Another application is that the PA gel can be used as a security paper for recording temporary information. We used an ice stick as a pen (ice pen), to write information on the surface of the PA gel. The temperature difference between the ice (0 °C) and the gel (25 °C) induces an obvious transparency change. Meanwhile, the contacting time between the ice and the surface of gel is very short (in the order of seconds), thus, the turbidity change only happens on the thin surface layer of the gel. This thin layer recovers to original appearance soon, resulting in a quick and autonomic disappearance of the recorded information (Fig. 8a). For example, we write a letter "L" on the surface of the gel; after 30 s, we write another letter "S", and L almost disappears at this time; then, we write a letter "W" after waiting for another 30 s, and S almost disappears; finally, W also disappears, and the PA gels turns to transparent as the original one (Fig. 8b and Movie S1).

Conclusion

In summary, we studied the thermoresponsive behavior of hydrogels containing abundance of physical bonds. We found that: (1) the structure frustration with a structure length on the micrometer scale is responsible for the transparent/opaque transition and asymmetric swelling/shrinking kinetics of the PA gel; (2) the small size change during the thermal response is due to the different temperature dependencies of ΔF_{mix}, ΔF_{ela}, and $\Delta F_{\mathrm{Coulombic}}$; (3) the cloud point depends on the cooling rate, owing

23

to the competition between the structure frustration and water diffusion; (4) the mechanical performances of the turbid gel and the transparent gel are similar, as a result of the negligible change in the skeleton bicontinuous network structure on the 60 nm scale of the gel, although the formation of nonequilibrium structure in μm scale. We also present two conceptual applications of this behavior in thermal imaging and security paper, albeit at a primitive level, suggesting the promising application of this new type of thermoresponsive material. This thermoresponsive behavior is universal for hydrogels containing an abundance of dynamic bonds, providing a wide choice for choosing gel chemistry. As this new type of thermoresponsive behavior enabled by nonequilibrium structure transformation has the advantages of thermal history dependence, quick and asymmetric thermal response, tunable cloud point and recovery time, tiny change in sample size and mechanical performance, we believe this type of hydrogels will be a promising thermoresponsive material. This work could also inspire future research on utilizing appropriately designed nonequilibrium structures to realize unique functionality.

Experimental Section

Materials. Cationic monomer, DMAEA-Q (79.2 *wt*%, MT AquaPolymer, Inc.), anionic monomer, NaSS (Wako Pure Chemical Industries, Ltd.), chemical cross-linker, *N,N'*-methylene-bis-acrylamide (MBAA; Wako Pure Chemical Industries, Ltd.), and ultraviolet (UV) initiator, α-ketoglutaric acid (α-keto; Wako Pure Chemical Industries, Ltd.) were used as received. Deionized water was used in all the

experiments.

Preparation of PA gels. The PA gels were synthesized with a concentrated aqueous solution containing anionic and cationic monomers at the charge balance point via one-step radical copolymerization, which has been described in detail in our previous work.[36] First, the prescribed amounts of anionic and cationic monomers (NaSS and DMAEA-Q), chemical crosslinker (MBAA), and initiator (α-keto) were dissolved in deionized water; then, the mixed solution was transferred into a sandwiched reaction cell consisting of two glasses separated by a silicone spacer, and irradiated with ultraviolet light (~365 nm) for 10 h in a glove box under an argon atmosphere. After copolymerization, the as-prepared gels were immersed in a sufficient amount of deionized water for 3 weeks to reach equilibrium. Silicone spacers with thickness of 1.5 and 0.1 mm were used in the preparation of the gel sheet and gel film, respectively.

Gel fraction and soluble fraction.

For simplicity, we did not consider the small ions, Na^+ and Cl^-. We recorded the masses of the total monomers m_1 (after subtracting Na^+ and Cl^-) and water m_2 in the precursor solution. After radical copolymerization, we submerged the gel in large amount of water and changed the water every day for two weeks to remove the soluble fraction. Then, we used a water balance moisture to obtain the mass of the dry polymer network, m_3. The mass of the soluble part is (m_1-m_3). The gel fraction, (m_3)/(m_1+m_2), and soluble fraction, (m_1-m_3)/(m_1+m_2), were 27.8 wt% and 4.5 wt%,

respectively.

Preparation of the PAAm gel. The PAAm hydrogel was synthesized by UV polymerization of a mixed solution containing 2 M acrylamide monomers, 1 mol% α-keto, and 0.1 mol% MBAA. A silicone spacer with a thickness of 1.5 mm was used. The other experimental procedures were the same as those of that of PA gel.

Transmittance measurement. The transmittance of the sample was characterized using a Shimadzu UV spectrophotometer (UV-1800) at a wavelength of 550 nm. The gel was placed in a quartz cuvette filled with water during measurement.

Microscopy measurement. A 3D violet laser scanning microscope (VK-8700, KEYENCE Co., Ltd.) was used to characterize the thickness of the thin PA gel film by step height measurements. The thickness of the thin hydrogel film is defined as the orthogonal distance between the two parallel planes representing the gel surface and substrate, respectively. Optical microscopy measurement was conducted with parallel polarizers (Olympus, BH-2) at room temperature. Optical images were captured by a digital camera coupled to the microscope.

Small-angle X-ray Scattering (SAXS) analysis. SAXS measurement was performed at the BL19U2 beamline of the National Facility for Protein Science (NFPS), Shanghai Synchrotron Radiation Facility (SSRF), Shanghai, China. The energy of X-

ray was 12 keV, and the sample-to-detector distance was 5934.0 mm. A Pilatus 1 M

detector with a resolution of 981×1043 pixels and the pixel size of 172×172 μm^2 was

used to record the 2D SAXS patterns. During measurement, the gel sample with a

thickness of 1.2 mm was loaded into a sample cell filled with water. The exposure

time for each sample was 0.1 s. The background scattering was measured with the

same configuration as the gel except that the gel was removed from the sample cell.

The 1D scattering profiles were obtained by integrating the 2D patterns *via* a Fit2D

software. The SAXS data were corrected for X-ray beam fluctuation, detector spatial

distortion, and background scattering. The temperature of the samples was controlled

by a Linkam THMS 600 hot stage.

Rheology test. Rheological measurement was performed using an ARES-G2

rheometer (TA Instruments, USA) with a parallel-plate geometry. Frequency sweep

measurement with frequency varying from 0.1 to 100 Hz was carried out with a strain

of 0.1 % at 25 °C. The disk-like sample with a diameter of 10 mm was adhered to the

parallel plates with a superglue and surrounded with deionized water during testing.

Uniaxial tensile test. Uniaxial tensile test was carried out at 25 °C with an Instron

5965 tensile tester (Instron Co.) under a water vapor atmosphere to avoid sample

dehydration. Samples with a gauge length of 12 mm, a width of 2mm, and a thickness

of 1.2 mm were used in this test. The tensile speed was 100 mm/min, which gave an

initial strain rate of 0.14 s^{-1}. Each sample was repeated 5 times to make an average.

27

Single-edge notch test. A single-edge notch test was performed under a water vapor atmosphere at 25 °C to obtain the fracture energy. Rectangular samples with a gauge length of 20 mm, width of 10 mm, and thickness of 1.2 mm, and with or without notch (length $c = 2$ mm) were used. The stretch speed was set at 100 mm/min. The fracture energy Γ was calculated by $\Gamma = 2\dfrac{3}{\sqrt{\lambda_c}}cW(\lambda_c)$, where $W(\lambda_c)$ is the strain energy density of an unnotched sample and λ_c is the stretch ratio where the crack starts to propagate for the notched sample. Each sample was repeated for 3 times to make an average.

Supporting Information

Supporting Information is available XXX. Additional experimental results, including the DSC result of the dry gel, transparent change during the thermal response, mechanical performance of the gel, and a movie to show the autonomic disappearance of the recorded temporary information.

Acknowledgments

Conflict of Interest

The authors declare no conflict of interest.

Keywords

Nonequilibrium, structure frustration, thermal history dependence, transient process,

self-healing hydrogels, dynamic bonds, transparency change, thermal imaging,

security paper

References

(1)   Freedman, B. R.; Mooney, D. J. Biomaterials to Mimic and Heal Connective Tissues. *Adv. Mater.* **2019**, *31* (19), 1–27.

(2)   SPENCER, M.; FULLER, W.; WILKINS, M. H. F.; BROWN, G. L. Determination of the Helical Configuration of Ribonucleic Acid Molecules by X-Ray Diffraction Study of Crystalline Amino-Acid–Transfer Ribonucleic Acid. *Nature* **1962**, *194* (4833), 1014–1020.

(3)   Teyssier, J.; Saenko, S. V.; van der Marel, D.; Milinkovitch, M. C. Photonic Crystals Cause Active Colour Change in Chameleons. *Nat. Commun.* **2015**, *6* (1), 6368.

(4)   Gorgoraptis, N.; Catalao, R. F. G.; Bays, P. M.; Husain, M. Dynamic Updating of Working Memory Resources for Visual Objects. *J. Neurosci.* **2011**, *31* (23), 8502–8511.

(5)   Nader, K. Memory Traces Unbound. *Trends Neurosci.* **2003**, *26* (2), 65–72.

(6)   Gong, J. P. Why Are Double Network Hydrogels so Tough? *Soft Matter* **2010**, *6* (12), 2583–2590.

(7)   Gong, J. P. Materials Both Tough and Soft. *Science (80-.).* **2014**, *344* (6180), 161–162.

(8)   Haque, M. A.; Kamita, G.; Kurokawa, T.; Tsujii, K.; Gong, J. P. Unidirectional

Alignment of Lamellar Bilayer in Hydrogel: One-Dimensional Swelling, Anisotropic Modulus, and Stress/Strain Tunable Structural Color. *Adv. Mater.* **2010**, *22* (45), 5110–5114.

(9) Lim, H. S.; Lee, J. H.; Walish, J. J.; Thomas, E. L. Dynamic Swelling of Tunable Full-Color Block Copolymer Photonic Gels via Counterion Exchange. *ACS Nano* **2012**, *6* (10), 8933–8939.

(10) Fu, F.; Shang, L.; Chen, Z.; Yu, Y.; Zhao, Y. Bioinspired Living Structural Color Hydrogels. *Sci. Robot.* **2018**, *3* (16), eaar8580.

(11) Guo, H.; Sanson, N.; Hourdet, D.; Marcellan, A. Thermoresponsive Toughening with Crack Bifurcation in Phase-Separated Hydrogels under Isochoric Conditions. *Adv. Mater.* **2016**, *28* (28), 5857–5864.

(12) Liu, M.; Ishida, Y.; Ebina, Y.; Sasaki, T.; Hikima, T.; Takata, M.; Aida, T. An Anisotropic Hydrogel with Electrostatic Repulsion between Cofacially Aligned Nanosheets. *Nature* **2015**, *517* (7532), 68–72.

(13) Wang, M.; Yin, Y. Magnetically Responsive Nanostructures with Tunable Optical Properties. *J. Am. Chem. Soc.* **2016**, *138* (20), 6315–6323.

(14) Haraguchi, K. Nanocomposite Hydrogels. *Curr. Opin. Solid State Mater. Sci.* **2007**, *11* (3–4), 47–54.

(15) Klein, A.; Whitten, P. G.; Resch, K.; Pinter, G. Nanocomposite Hydrogels: Fracture Toughness and Energy Dissipation Mechanisms. *J. Polym. Sci. Part B Polym. Phys.* **2015**, *53* (24), 1763–1773.

(16) Nonoyama, T.; Lee, Y. W.; Ota, K.; Fujioka, K.; Hong, W.; Gong, J. P. Instant Thermal Switching from Soft Hydrogel to Rigid Plastics Inspired by Thermophile Proteins. *Adv. Mater.* **2020**, *32* (4), 1905878.

(17) Yu, C.; Guo, H.; Cui, K.; Li, X.; Ye, Y. N.; Kurokawa, T.; Gong, J. P. Hydrogels as Dynamic Memory with Forgetting Ability. *Proc. Natl. Acad. Sci. U. S. A.* **2020**, *117* (32), 18962–18968.

(18) Zhu, C.-H.; Lu, Y.; Peng, J.; Chen, J.-F.; Yu, S.-H. Photothermally Sensitive Poly(N -Isopropylacrylamide)/Graphene Oxide Nanocomposite Hydrogels as Remote Light-Controlled Liquid Microvalves. *Adv. Funct. Mater.* **2012**, *22* (19), 4017–4022.

(19) Kim, Y. S.; Liu, M.; Ishida, Y.; Ebina, Y.; Osada, M.; Sasaki, T.; Hikima, T.; Takata, M.; Aida, T. Thermoresponsive Actuation Enabled by Permittivity Switching in an Electrostatically Anisotropic Hydrogel. *Nat. Mater.* **2015**, *14* (10), 1002–1007.

(20) Lu, W.; Le, X.; Zhang, J.; Huang, Y.; Chen, T. Supramolecular Shape Memory Hydrogels: A New Bridge between Stimuli-Responsive Polymers and Supramolecular Chemistry. *Chem. Soc. Rev.* **2017**, *46* (5), 1284–1294.

(21) Kuang, X.; Roach, D. J.; Wu, J.; Hamel, C. M.; Ding, Z.; Wang, T.; Dunn, M. L.; Qi, H. J. Advances in 4D Printing: Materials and Applications. *Adv. Funct. Mater.* **2019**, *29* (2), 1805290.

(22) Liu, K.; Zhang, Y.; Cao, H.; Liu, H.; Geng, Y.; Yuan, W.; Zhou, J.; Wu, Z. L.; Shan, G.; Bao, Y.; Zhao, Q.; Xie, T.; Pan, P. Programmable Reversible Shape Transformation of Hydrogels Based on Transient Structural Anisotropy. *Adv.*

Mater. **2020**, *32* (28), 2001693.

(23) Zhao, F.; Zhou, X.; Liu, Y.; Shi, Y.; Dai, Y.; Yu, G. Super Moisture-Absorbent Gels for All-Weather Atmospheric Water Harvesting. *Adv. Mater.* **2019**, *31* (10), 1806446.

(24) Roy, D.; Brooks, W. L. A.; Sumerlin, B. S. New Directions in Thermoresponsive Polymers. *Chem. Soc. Rev.* **2013**, *42* (17), 7214.

(25) Dompé, M.; Cedano-Serrano, F. J.; Heckert, O.; van den Heuvel, N.; van der Gucht, J.; Tran, Y.; Hourdet, D.; Creton, C.; Kamperman, M. Thermoresponsive Complex Coacervate-Based Underwater Adhesive. *Adv. Mater.* **2019**, *31* (21), 1808179.

(26) Seuring, J.; Agarwal, S. Polymers with Upper Critical Solution Temperature in Aqueous Solution. *Macromol. Rapid Commun.* **2012**, *33* (22), 1898–1920.

(27) Asadujjaman, A.; Kent, B.; Bertin, A. Phase Transition and Aggregation Behaviour of an UCST-Type Copolymer Poly(Acrylamide-Co-Acrylonitrile) in Water: Effect of Acrylonitrile Content, Concentration in Solution, Copolymer Chain Length and Presence of Electrolyte. *Soft Matter* **2017**, *13* (3), 658–669.

(28) Fu, W.; Zhao, B. Thermoreversible Physically Crosslinked Hydrogels from UCST-Type Thermosensitive ABA Linear Triblock Copolymers. *Polym. Chem.* **2016**, *7* (45), 6980–6991.

(29) Erol, O.; Pantula, A.; Liu, W.; Gracias, D. H. Transformer Hydrogels: A Review. *Adv. Mater. Technol.* **2019**, *4* (4), 1900043.

(30) Ye, Z.; Sun, S.; Wu, P. Distinct Cation–Anion Interactions in the UCST and LCST Behavior of Polyelectrolyte Complex Aqueous Solutions. *ACS Macro Lett.* **2020**, *9* (7), 974–979.

(31) Gibson, M. I.; Paripovic, D.; Klok, H.-A. Size-Dependent LCST Transitions of Polymer-Coated Gold Nanoparticles: Cooperative Aggregation and Surface Assembly. *Adv. Mater.* **2010**, *22* (42), 4721–4725.

(32) Zhang, X.-Z.; Zhang, J.-T.; Zhuo, R.-X.; Chu, C.-C. Synthesis and Properties of Thermosensitive, Crown Ether Incorporated Poly(N-Isopropylacrylamide) Hydrogel. *Polymer (Guildf).* **2002**, *43* (17), 4823–4827.

(33) Yan, Q.; Hoffman, A. S. Synthesis of Macroporous Hydrogels with Rapid Swelling and Deswelling Properties for Delivery of Macromolecules. *Polymer (Guildf).* **1995**, *36* (4), 887–889.

(34) Pei, D.; Luan, J. Development of Visible Light-Responsive Sensitized Photocatalysts. *Int. J. Photoenergy* **2012**, *2012*, 1–13.

(35) Echeverria, C.; López, D.; Mijangos, C. UCST Responsive Microgels of Poly(Acrylamide−acrylic Acid) Copolymers: Structure and Viscoelastic Properties. *Macromolecules* **2009**, *42* (22), 9118–9123.

(36) Sun, T. L.; Kurokawa, T.; Kuroda, S.; Ihsan, A. Bin; Akasaki, T.; Sato, K.; Haque, M. A.; Nakajima, T.; Gong, J. P. Physical Hydrogels Composed of Polyampholytes Demonstrate High Toughness and Viscoelasticity. *Nat. Mater.* **2013**, *12* (10), 932–937.

(37) Wu, S.; Shao, Z.; Xie, H.; Xiang, T.; Zhou, S. Salt-Mediated Triple Shape-Memory Ionic Conductive Polyampholyte Hydrogel for Wearable Flexible

Electronics. *J. Mater. Chem. A* **2021**, *9* (2), 1048–1061.

(38) Cui, K.; Ye, Y. N.; Yu, C.; Li, X.; Kurokawa, T.; Gong, J. P. Stress Relaxation and Underlying Structure Evolution in Tough and Self-Healing Hydrogels. *ACS Macro Lett.* **2020**, *9*, 1582–1589.

(39) Cui, K.; Ye, Y. N.; Sun, T. L.; Yu, C.; Li, X.; Kurokawa, T.; Gong, J. P. Phase Separation Behavior in Tough and Self-Healing Polyampholyte Hydrogels. *Macromolecules* **2020**, *53* (13), 5116–5126.

(40) Cui, K.; Ye, Y. N.; Sun, T. L.; Chen, L.; Li, X.; Kurokawa, T.; Nakajima, T.; Nonoyama, T.; Gong, J. P. Effect of Structure Heterogeneity on Mechanical Performance of Physical Polyampholytes Hydrogels. *Macromolecules* **2019**, *52* (19), 7369–7378.

(41) Cui, K.; Sun, T. L.; Liang, X.; Nakajima, K.; Ye, Y. N.; Chen, L.; Kurokawa, T.; Gong, J. P. Multiscale Energy Dissipation Mechanism in Tough and Self-Healing Hydrogels. *Phys. Rev. Lett.* **2018**, *121* (18), 185501.

(42) Li, X.; Cui, K.; Sun, T. L.; Meng, L.; Yu, C.; Li, L.; Creton, C.; Kurokawa, T.; Gong, J. P. Mesoscale Bicontinuous Networks in Self-Healing Hydrogels Delay Fatigue Fracture. *Proc. Natl. Acad. Sci.* **2020**, *117* (14), 7606–7612.

(43) Xu, S.; Scherer, G. W.; Mahadevan, T. S.; Garofalini, S. H. Thermal Expansion of Confined Water. *Langmuir* **2009**, *25* (9), 5076–5083.

(44) Hoshino, K. I.; Nakajima, T.; Matsuda, T.; Sakai, T.; Gong, J. P. Network Elasticity of a Model Hydrogel as a Function of Swelling Ratio: From Shrinking to Extreme Swelling States. *Soft Matter* **2018**, *14* (47), 9693–9701.

(45) English, A. E.; Mafé, S.; Manzanares, J. A.; Yu, X.; Grosberg, A. Y.; Tanaka, T. Equilibrium Swelling Properties of Polyampholytic Hydrogels. *J. Chem. Phys.* **1996**, *104* (21), 8713–8720.

(46) Malmberg, C. G.; Maryott, A. A. Dielectric Constant of Water from 0 to 100 C. *J. Res. Natl. Bur. Stand. (1934).* **1956**, *56* (1), 1–8.

(47) Bai, R.; Yang, J.; Morelle, X. P.; Suo, Z. Flaw-Insensitive Hydrogels under Static and Cyclic Loads. *Macromol. Rapid Commun.* **2019**, *40* (8), 1800883.

For Table of content use only

Structure Frustration Enables Thermal History-Dependent Responsive Behavior in Self-Healing Hydrogels

Chengtao Yu[a,b], Kunpeng Cui[c]*, Honglei Guo[d], Ya Nan Ye[e], Xueyu Li[e], and Jian Ping Gong[c,d,e]*